J Electroceram
DOI 10.1007/s10832-014-9977-2

Facile preparation of a Nb_2O_5 blocking layer for dye-sensitized solar cells

Sung-Hwan Lim · Kwang-Won Park · Ming Hao Jin · Sungwoo Ahn · Jeemin Song · Jongin Hong

Received: 6 August 2014 / Accepted: 29 October 2014
© Springer Science+Business Media New York 2014

Abstract The introduction of a niobium oxide layer between fluorine-doped tin oxide (FTO) and TiO_2 electrodes is known to enhance the power conversion efficiency (η) of dye-sensitized solar cells (DSSCs). Nb thin films were deposited on FTO glass substrates using RF magnetron sputtering. TiO_2 pastes were then screen-printed onto the Nb thin films. The multilayered structures were annealed at 500 °C in a muffle furnace and assembled with Pt counter electrodes for DSSC performance evaluation. The Nb thin films were oxidized during the calcination process, producing a post-oxidized layer that increased the solar-cell efficiency by about 15 % and the photocurrent density by approximately 25 %.

Keywords Nb2O5 · Blocking layer · Sputtering · Dye-sensitized solar cells

1 Introduction

Over the last few decades, dye-sensitized solar cells (DSSCs) have attracted significant academic and commercial attention as low-cost alternatives to conventional solid-state photovoltaic devices [1–3]. Many researchers in both academia and industry have endeavored to improve the performance of DSSCs for further commercialization including the development of building- or vehicle-integrated photovoltaic applications (BIPV or VIPV). General DSSCs contain many interfaces, including the fluorine-doped tin oxide (FTO)/TiO_2 photoanode, TiO_2 photoanode/photosensitizer, photosensitizer/electrolyte, and electrolyte/counter electrode interfaces, which are crucial to cell performance. Unidirectional charge flow with minimal charge leakage guarantees high power conversion efficiency (η) in DSSCs. Several approaches to achieving this goal, termed called interface engineering strategies, have been recently reported [4, 5].

Prevention of charge recombination at the FTO/TiO_2 interface in the liquid electrolyte of DSSCs is of significant importance, as the interface is the site of reaction between photo-injected electrons and I_3^- ions. A previous study introduced a TiO_2 compact layer at the FTO/TiO_2 interface as a blocking layer. However, the blocking layer did not dramatically improve their power conversion efficiency, and the approach was not widely adopted. Recently, however, Peter *et al*. sparked significant interest in the development of novel blocking layers, describing the crucial mechanistic role of the TiO_2 blocking layer the prevention of back-electron transfer [6, 7]. Yanagida and co-workers evaluated different oxides as potential blocking materials [8], and reported that Nb_2O_5 thin films enhance both the open-circuit voltage (V_{oc}) and fill factor (FF) due to the potential barrier created between the Nb_2O_5 and TiO_2 layers [9].

To date, such Nb_2O_5 blocking layers have been prepared by spray pyrolysis [9], reactive sputtering [10, 11] and the sol–gel method [12]. The sputtering method offers several advantages over the other methods, including source material diversity, uniform deposition, good reproducibility, compatibility with reactive gases and suitability for large-scale production. However, the relative pressures of the inert and reactive gases in the reactive sputtering affect film stoichiometry and thickness and, in turn, DSSC performance. To address this issue, we propose a simple method to obtain the niobium oxide blocking layer through thermal oxidation of a metallic niobium film during the DSSC fabrication (Scheme 1). Following the deposition of the metallic niobium film on the transparent FTO conducting substrates, further ex-situ annealing for the

Sung-Hwan Lim and Kwang-Won Park have equal contribution to this article

S.-H. Lim · K.-W. Park · M. H. Jin · S. Ahn · J. Song · J. Hong (✉)
Department of Chemistry, Chung-Ang University, Seoul 156-756, South Korea
e-mail: hongj@cau.ac.kr

Published online: 30 November 2014

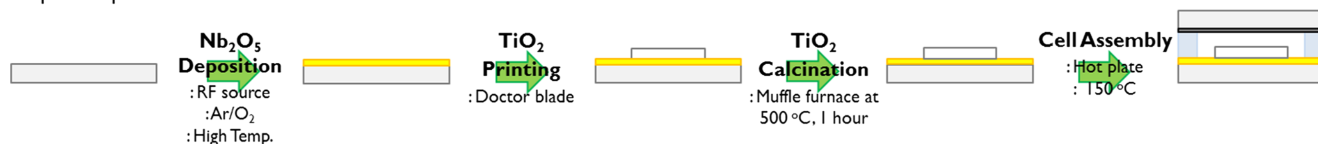

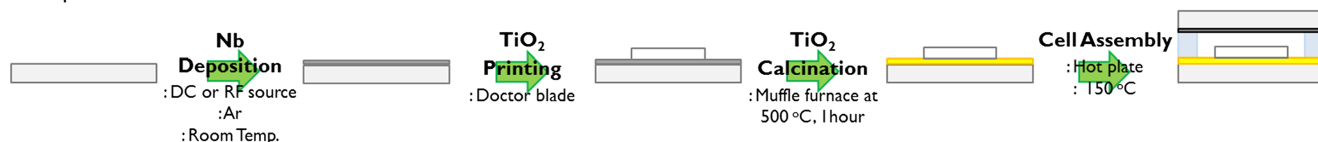

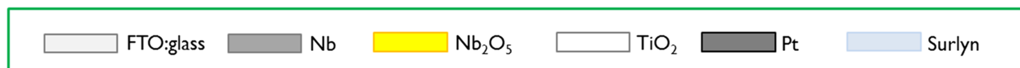

Scheme 1 Entire cell assembly procedure

fabrication of nanoporous TiO_2 electrodes at elevated temperature in air was allowed to simultaneously form niobium oxide films.

2 Experimental

Niobium deposition & thermal oxidation Anhydride ethanol, acetone, isopropyl alcohol and other materials were purchased from Sigma Aldrich and used without further purification. All substrates were serially cleaned in acetone, isopropyl alcohol and deionized water by ultrasonication and dried with compressed nitrogen gas. High-purity metallic Nb targets (99.999 % in purity, 76 mm in diameter) were purchased from iTasco, Korea. Nb-modified FTO substrates were fabricated by Nb deposition onto transparent FTO conducting glass (Tec 8, Pilkington, 2.3 mm-thickness, sheet resistance of 8 Ω/□). Nb films of different thicknesses were deposited on the substrates at room temperature by radio-frequency (RF) magnetron sputtering with pure Ar gas using the Nb target. The base pressure was below 6.5×10^{-7} Torr, and the working pressure was maintained at 10 mtorr, with an Ar gas flow rate of 50 sccm. The RF power was 50 W, and the distance between the Nb target and the substrate holder was 6 cm. The Nb deposition rate was 3 nm/min, and the film thickness was controlled by adjusting deposition time. Thermal oxidation of metallic Nb thin films was carried out for 1 h at 500 °C in a muffle furnace. It should be noted that the oxidation conditions are the same as the calcination conditions for TiO_2 thick films used in the fabrication of DSSCs.

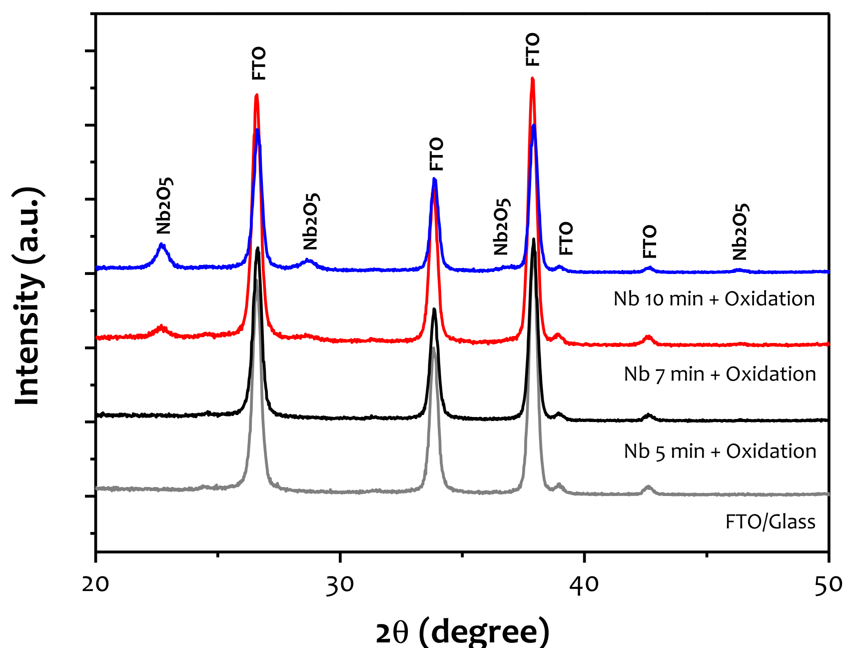

Fig. 1 XRD patterns of FTO and Nb-modified FTO annealed at 500 °C

Characterization The crystalline orientation was determined by X-ray diffraction (XRD, D/MAX-RC, Rigaku, Japan) with a 2θ scan at 40 kV, 100 mA. The optical transmittance spectra were collected with a UV/Vis/NIR spectrophotometer (V-670, JASCO, USA) at wavelengths from 300 to 1200 nm. The excitation and photoluminescence (PL) spectra were measured with a photoluminescence spectrometer (iHR320, HORIBA Ltd., France). The excitation wavelength was 300 nm. Cross sectional images were obtained using a field-emission scanning electron microscope (FE-SEM, Sirion, FEI, Netherlands). Energy-dispersive X-ray spectroscopy (EDS) was used to determine the chemical composition of thin films. X-ray photoelectron spectroscopy (XPS) measurements were carried out with a K-alpha XPS system (Thermo Fisher Scientific Inc.) using a monochromated Al Kα X-ray source with an energy of 1486.6 eV. Survey spectra were collected in the energy range between 0 and 1000 eV at 1 eV/step. The spectra of the Nb 3d and O 1s peaks were calibrated with respect to the C 1s peak at 248.8 eV of the surface adventitious carbon. XPS depth profiling was performed in the same system. The surface was bombarded with 3 keV Ar^+ ions and the argon beam was rastered over an area of 2×2 mm^2 around the point of impact of the ion beam.

DSSC fabrication & characterization TiO_2 powders (P25, 80 % anatase (d=21 nm) and 20 % rutile (d=50 nm)) were purchased from Degussa, Germany. The powders (6 g) were mixed with acetic acid (1 mL) and ethanol (30 mL) and the solution was ground in a mortar for 1 h to break down large TiO_2 aggregates. The TiO_2 dispersions were mixed with anhydrous terpinol (20 g) and 10 % ethylcellulose. The mixture was stirred by a magnetic bar and sonicated using an ultrasonic horn (Misonix XL2020, USA). The mixed paste was concentrated at 80 °C for 2 h on a rotary evaporator to obtain the appropriate viscosity for screen printing. The TiO_2 paste was printed on Nb-modified FTO conducting glass (Tec 8, 2.3 mm-thickness, sheet resistance: 8 Ω/□, Pilkington) by the doctor blade technique. The printed film was calcined at 500 °C for 1 h in a muffle furnace to remove organic compounds and to improve the interconnection among TiO_2 nanoparticles. The thickness and active area of the electrodes were 7 µm and 0.25 cm^2, respectively. The prepared TiO_2 electrodes were immersed in a 0.04 M $TiCl_4$ solution at 70 °C for 1 h, gently rinsed with water and then annealed on a hot plate at 500 °C for 30 min. The photoanodes were exposed to O_2 plasma (VITA, FEMTO science, Korea), and then immersed into a 0.5 mM photosensitizer solution in ethanol ((cis-diisothiocyanato-bis(2,2-bipyridyl-4,4′-dicarboxylato) ruthenium(II) bis-(tetrabutylammonium), N-719, Solaronix) for 24 h. A Pt counter electrode was prepared by magnetron sputtering on a FTO glass, in which two holes had been drilled. Both the TiO_2 photoanode and the Pt counter electrode were assembled with a hot-melt gasket of 60 µm-thick Surlyn (Solaronix). A liquid electrolyte (Iodolyte AN-50, Solaronix) was injected into the hole on the backside of the counter

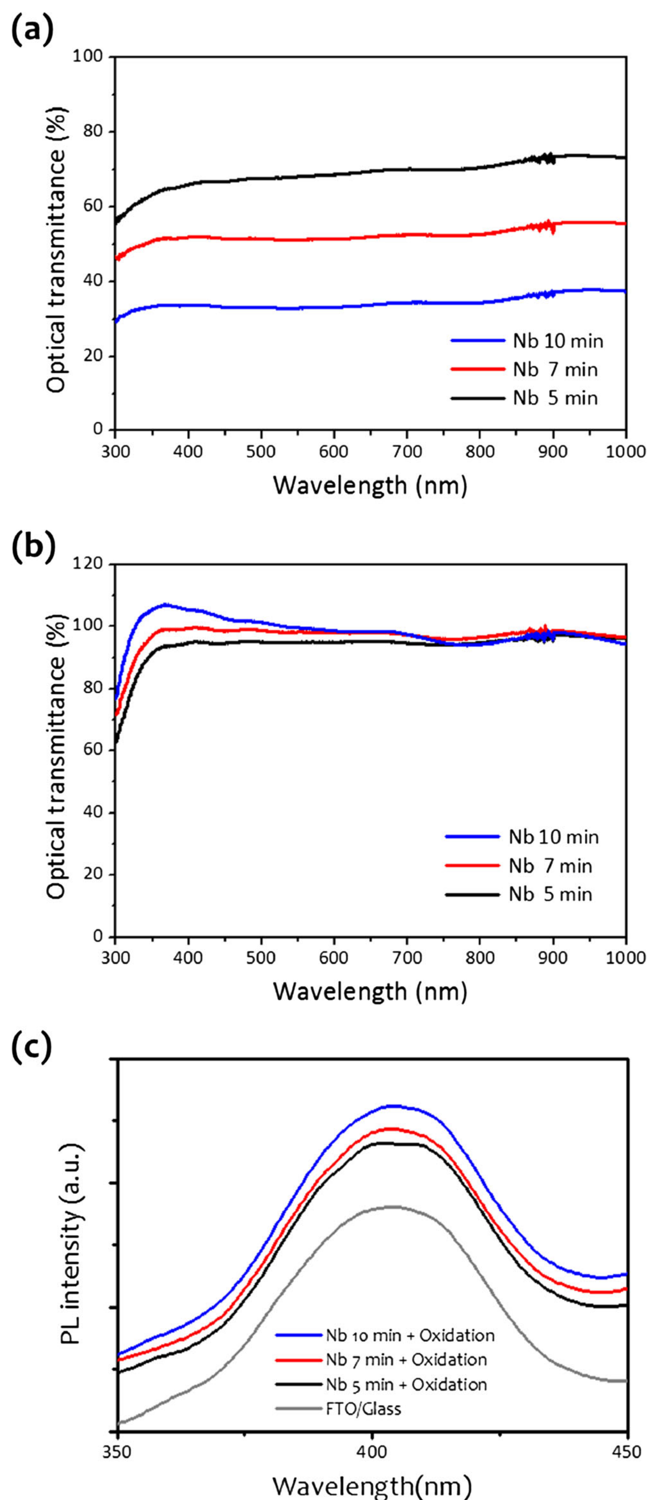

Fig. 2 Optical transmittance of Nb thin films (**a**) before and (**b**) after post-annealing at 500 °C and (**c**) emission spectra of the post-annealed films on FTO under excitation at 300 nm

electrode. The photovoltaic characteristics of the solar cells under Air Mass 1.5 Global (AM 1.5 G) 1-sun illumination (100 mW/m^2) were investigated using a solar cell I-V measurement system (K3000 LAB, McScience, Korea). The light intensity was calibrated with a reference cell (K801, McScience, Korea). The photocurrent density (J_{sc}), open-circuit voltage (V_{oc}), fill factor (FF) and power-conversion-efficiency (η) were measured simultaneously.

3 Results and discussion

XRD analysis Figure 1 shows XRD patterns of Nb-modified FTO glass substrates after annealing at 500 °C in the muffle furnace. The bare FTO/glass showed main peaks at 2θ=26.6° (110), 33.9° (101), 37.9° (200), 39.0° (111), 42.6° (210), 51.8° (211), 54.7° (220), and 57.8° (002) (JCPDS no. 77–0448). The hexagonal phase of Nb_2O_5 showed peaks at 2θ=22.6° (001), 28.6° (100), 36.7° (101) and 46.2° (002) (JCPDS no. 28–317). As the thickness of the initial Nb thin films increased, characteristic peaks of orthorhombic Nb_2O_5 appeared and their intensities increased. As a typical n-type, wide bandgap semiconductor (E_g=3.4 eV), Nb_2O_5 is the most thermodynamically stable phase among the various niobium oxides [13]. This indicates that the post-annealing treatment converts metallic Nb to crystalline Nb_2O_5 well, despite volume expansion due to Nb-O bonding.

Optical transmittance & photoluminescence During DSSC operation, light passes through glass, a FTO layer and a blocking layer before reaching the photosensitizers. Thus, it is important to consider the optical properties of the blocking layer, which is Nb_2O_5, in the present case. The transmittance spectra of Nb-modified FTO glass substrates before and after post-annealing at 500 °C are shown in Fig. 2(a) and (b), respectively. The transmittance of metallic Nb films did not change a lot as the wavelength increased. The light absorbance of the metallic films is related to radiation-stimulated intraband electron transitions within the metals, which contain partially filled d-shells within their electronic structure. In accordance with the Beer-Lambert law, the transmittance of the Nb thin films decreased as the film thickness increased. However, thermal oxidation of the metallic Nb films improved the optical transparency in the visible light region. Such improved transparency results from less reflectance of the incident light at the FTO/Nb_2O_5 and Nb_2O_5/air interfaces due to the high refractive index of Nb_2O_5 (e.g. n(FTO) = 1.74 and n(Nb_2O_5) = 2.32 at 632.8 nm) (http://www.filmetrics.com/refractive-index-database). For instance, the reflectivity (R) at normal incidence for any absorbing media of large optical band-gap can be expressed as

$$R = \frac{(n_1 - n_2)^2}{(n_1 + n_2)^2} \qquad (1)$$

where n_m is the refractive index of m (=1, 2) [14]. Moreover, as the wavelength of the incident light decreases, the values of n(FTO) decrease but those of n(Nb_2O_5) increase (http://www.filmetrics.com/refractive-index-database) [15]. This indicates that the reflectivity becomes weaker as the wavelength of the incident light is near ultraviolet. Additionally, the less reflectance of the incident light, implying more penetrating light, may result in the increase in the total internal reflection in the FTO/Nb_2O_5/air waveguide structure. The total internal reflection allows for the appearance of an evanescent wave beyond the boundary interfaces. We think that such evanescent wave could stimulate FTO films and thus enhance their photoluminescence (Fig. 2c). The prominent emission

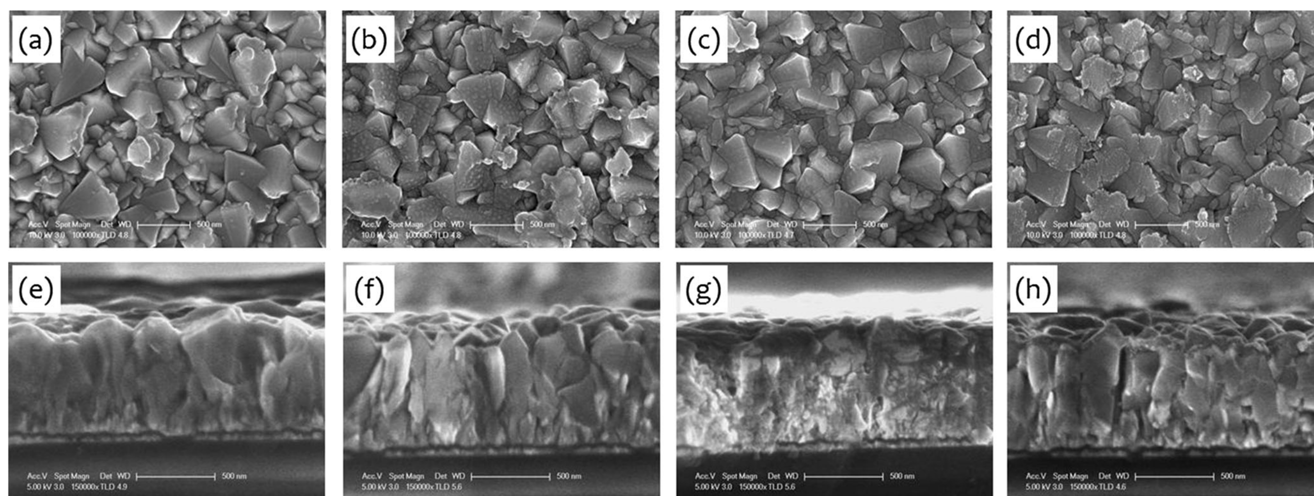

Fig. 3 SEM surface and cross-sectional images: (**a** and **e**) FTO, (**b** and **f**) Nb sputtering for 5 min and calcination at 500 °C, (**c** and **g**) Nb sputtering for 7 min and calcination at 500 °C, (**d** and **h**) Nb sputtering for 10 min and at 500 °C

centered at 400 nm stems from electron transition mediated by defect levels associated with oxygen vacancies or tin interstitials, which can act as radiative centers in luminescence processes [16].

SEM Figure 3 shows SEM images of bare FTO (Fig. 3a and e) and Nb_2O_5 films on FTO (Fig. 3b–d and f–h). Both top-view (Fig. 3a–d) and cross-sectional (Fig. 3e–h) images are shown. The bare FTO surface exhibited morphology characteristic of tin oxide crystals, with particle sizes between 300 and 450 nm (Fig. 3a) and its thickness of 796±47 nm, as shown in the corresponding cross-sectional image (Fig. 3e). After 5 min of sputtering and thermal oxidation, small islands of Nb_2O_5 (30~50 nm diameter) were homogeneously distributed on the surface of FTO (Fig. 3b). As the Nb_2O_5 film grew thicker, the rough surface of bare FTO began to smoothen as the growing layer of Nb_2O_5 softened the sharp edges of underlying FTO crystals (Fig. 3c–d). This is illustrated by the cross-sectional images (Fig. 3f–h), where the Nb_2O_5 surface is smoothed to an appreciable extent but still reflects the underlying FTO morphology. Dense and continuous Nb_2O_5 films were obtained after 10 min of sputtering and thermal oxidation (Fig. 3h), displaying a final thickness of approximately 852±42 nm.

XPS depth profile Figure 4 shows the variation in the relative concentration of the main components (O 1s, Nb 3d, F 1s, Sn 3d) of the Nb_2O_5 films on FTO as a function of sputtering depth. Niobium oxide was observed at the near-surface region. The atomic concentration of Nb monotonically decreased as digging down from the surface, whilst that of Sn increased to its original atomic concentration in pure FTO. Interestingly, the Nb atoms diffused into the FTO layer even after etching 100 nm or more. These data coincide with EDS results as shown in Fig. 5. A very low concentration of fluorine was detected throughout the depth of the film.

J-V characteristics Figure 6 shows the J-V characteristics of DSSCs fabricated on the Nb-modified FTO glass. The photovoltaic parameters are summarized in Table 1. Increases in Nb deposition time improved the photovoltaic performance: J_{sc} increased from 10.1 mA/cm^2 (TiO_2 only) to 12.6 mA/cm^2 and η increased from 4.91 % (TiO_2 only) to 5.60 %. The introduction of the Nb_2O_5 layer at the interface of FTO and nanocrystalline TiO_2 layers forms 100 mV potential barriers [17], suppressing electron leakage between the two layers and increasing the photo-current density. The efficient usage of incident light (less reflection, more internal reflection and more photoluminescence) might also be responsible for the increase in current density.

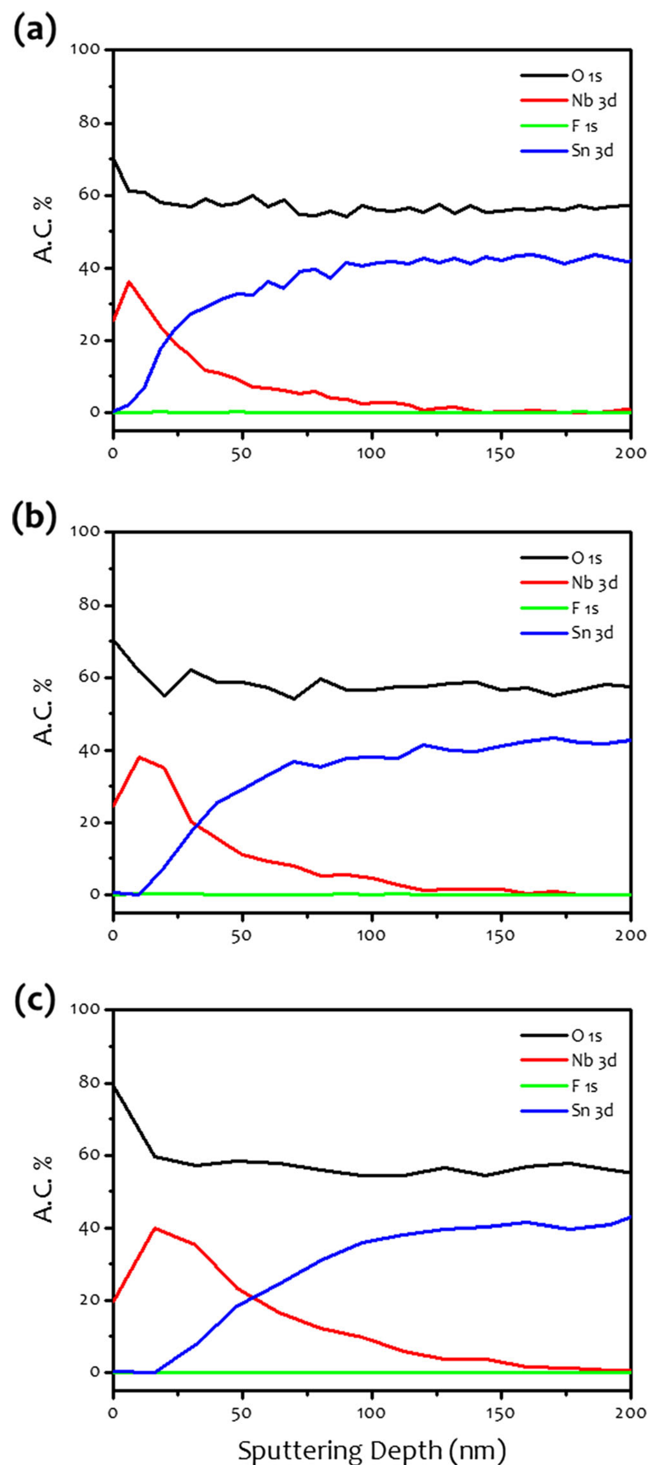

Fig. 4 XPS depth profiles of Nb-modified FTO annealed at 500 °C: Nb sputtering for (**a**) 5 min, (**b**) 7 min and (**c**) 10 min

4 Conclusion

In contrast to the typical method of Nb_2O_5 thin film deposition on FTO, Nb thin films were deposited on FTO substrates by RF magnetron sputtering, followed

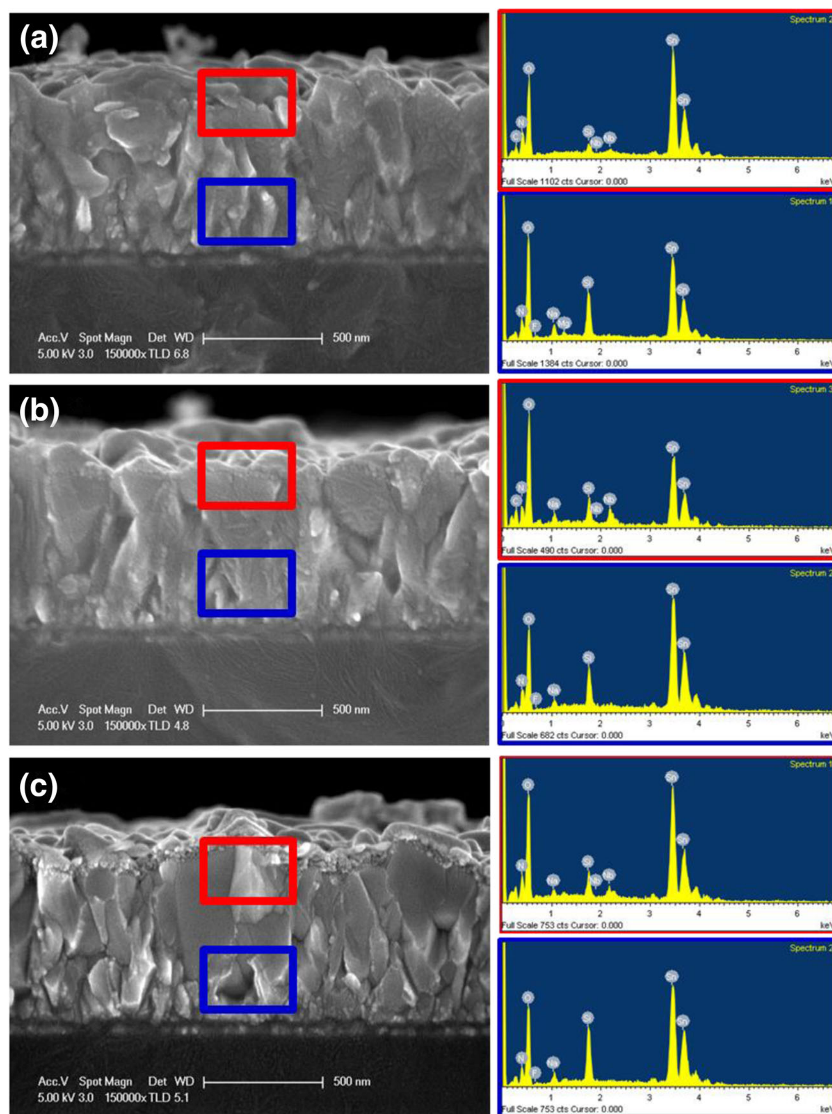

Fig. 5 SEM cross-sectional images and EDS analysis of Nb-modified FTO annealed at 500 °C: Nb sputtering for (**a**) 5 min, (**b**) 7 min and (**c**) 10 min

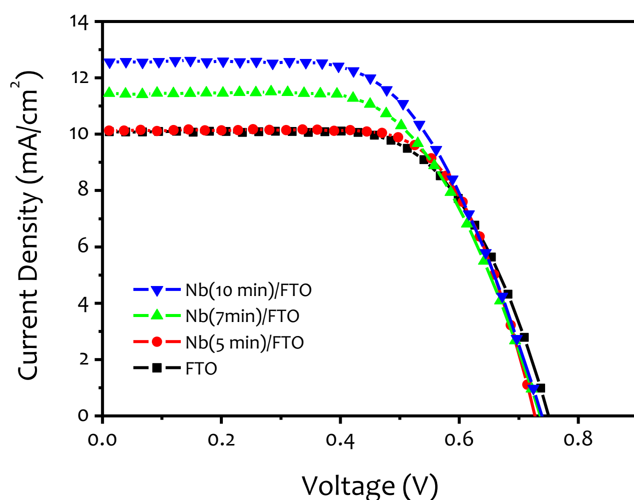

Fig. 6 J-V characteristics of DSSCs with 7.0 μm-thick TiO_2 photoanode on FTO and Nb-modified FTO substrates under AM 1.5 G 1-sun illumination

by screening-printing of TiO_2 photoanodes and calcination. The Nb thin films were oxidized during the calcination process and the resulting oxidized layer improved the photovoltaic performance of DSSCs. The formation of a blocking layer between the FTO and the nanocrystalline TiO_2 layers enhanced the solar-cell efficiency from 4.91 % (TiO_2 only) to 5.60 % and the photocurrent density from 10.2 mA/cm^2 (TiO_2 only) to 12.8 mA/cm^2.

Table 1 Photovoltaic performance of DSSCs

Substrate	V_{oc} (V)	J_{sc} (mA/cm^2)	FF (%)	η (%)
FTO	0.75	10.1	65.0	4.91
Nb(5 min)+FTO	0.73	10.1	68.5	5.06
Nb(7 min)+FTO	0.74	11.1	61.5	5.18
Nb(10 min)+FTO	0.74	12.6	60.3	5.60

Acknowledgments This research was supported by the Chung-Ang University Research Scholarship Grants in 2012, the Basic Science Research Program (2013-026989) through the National Research Foundation (NRF) funded by the Ministry of Science, ICT & Future Planning (MSIP) of Korea.

References

1. R. Jose, V. Thavasi, S. Ramakrishna, J. Am. Ceram. Soc. **92**, 289 (2009)
2. A. Hagfeldt, G. Boschloo, L. Sun, L. Kloo, H. Petterson, Chem. Rev. **110**, 6595 (2010)
3. B.E. Hardin, H.J. Snaith, M.D. McGehee, Nat. Photonics **6**, 163 (2012)
4. B.A. Gregg, Coord. Chem. Rev. **248**, 1215 (2004)
5. J. Xia, S. Yanagida, Sol. Energy **85**, 3143 (2011)
6. P.J. Cameron, L.M. Peter, S. Hore, J. Phys. Chem. B **109**, 930 (2005)
7. P.J. Cameron, L.M. Peter, J. Phys. Chem. B **109**, 7392 (2005)
8. J.H. Yum, S. Nakade, D.Y. Kim, S. Yanagida, J. Phys. Chem. B **110**, 3215 (2006)
9. J. Xia, N. Masaki, K. Jiang, S. Yanagida, J. Photochem. Photobiol. A **188**, 120 (2007)
10. J. Xia, N. Masaki, K. Jiang, S. Yanagida, Chem. Commun. **138** (2007)
11. J. Xia, N. Masaki, K. Jiang, S. Yanagida, J. Phys. Chem. C **111**, 8092 (2007)
12. T.Y. Cho, K.W. Ko, S.G. Yoo, S.S. Sekhon, M.G. Kang, Y.S. Hong, C.H. Han, Curr. Appl. Phys. **13**, 1391 (2013)
13. G. Agarwal, G.B. Reddy, J. Mater. Sci. Eng. **16**, 21 (2005)
14. J. Hong, Y. Lee, G.A.T. Chansin, J.B. Edel, A.J. deMello, Nanotechnology **19**, 165205 (2008). 8pp
15. H.H. Afify, R.S. Momtaz, W.A. Badawy, S.A. Nasser, J. Mater. Sci. Eng. **2**, 40 (1991)
16. F. Gu, S.F. Wang, M.K. Lü, G.J. Zhou, D. Xu, D.R. Yuan, J. Phys. Chem. B **108**, 8119 (2004)
17. K. Sayama, H. Sugihara, H. Arakawa, Chem. Mater. **10**, 3825 (1998)